NPY-Y1 receptor signaling controls spatial learning and perineuronal net expression

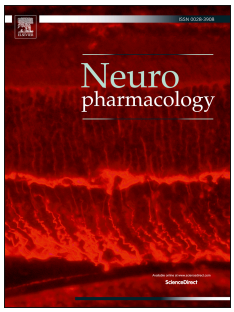

NPY-Y1 receptor signaling controls spatial learning and perineuronal net expression

Ilaria Bertocchi, Paolo Mele, Giuliano Ferrero, Alessandra Oberto, Daniela Carulli, Carola Eva

PII: S0028-3908(20)30493-7

DOI: https://doi.org/10.1016/j.neuropharm.2020.108425

Reference: NP 108425

To appear in: *Neuropharmacology*

Received Date: 19 June 2020

Revised Date: 24 November 2020

Accepted Date: 1 December 2020

Please cite this article as: Bertocchi, I., Mele, P., Ferrero, G., Oberto, A., Carulli, D., Eva, C., NPY-Y1 receptor signaling controls spatial learning and perineuronal net expression, *Neuropharmacology* (2021), doi: https://doi.org/10.1016/j.neuropharm.2020.108425.

Bertocchi Ilaria: Conceptualization, Data curation, Writing - original draft, Writing - review & editing; Mele Paolo: Conceptualization, Data curation, Writing - original draft, Writing - review & editing; Ferrero Giuliano: Investigation, Data curation; Oberto Alessandra: Data curation; Carulli Daniela: Supervision, Conceptualization, Data curation, Writing - original draft, Writing - review & editing; Eva Carola: Funding acquisition, Supervision, Conceptualization, Data curation, Writing - original draft, Writing - review & editing.

NPY-Y1 RECEPTOR SIGNALING CONTROLS SPATIAL LEARNING AND PERINEURONAL NET EXPRESSION

Ilaria Bertocchi[abc1], Paolo Mele[ab1], Giuliano Ferrero[a], Alessandra Oberto[abc], Daniela Carulli[abcd2], Carola Eva[abc2]

Affiliations: [a]Neuroscience Institute of the Cavalieri-Ottolenghi Foundation, 10043 Orbassano (Turin), Italy; [b]Department of Neuroscience, University of Turin, 10126 Turin, Italy;

[c]Neuroscience Institute of Turin; [d]Netherlands Institute for Neuroscience, 1105 BA Amsterdam, Netherlands.

[1] Shared first authors

[2] Shared last authors

Corresponding author: Carola Eva, Ph.D., Neuroscience Institute of the Cavalieri-Ottolenghi Foundation (NICO), Regione Gonzole 10, University of Turin, 10043 Orbassano (Turin), Italy. Email: carola.eva@unito.it

Abstract

Perineuronal nets (PNNs) are extracellular matrix structures that form around some types of neurons at the end of critical periods, limiting neuronal plasticity. In the adult brain, PNNs play a crucial role in the regulation of learning and cognitive processes. Neuropeptide Y (NPY) is involved in the regulation of many physiological functions, including learning and memory abilities, via activation of Y1 receptors (Y1Rs). Here we demonstrated that the conditional depletion of the gene encoding the Y1R for NPY in adult forebrain excitatory neurons (Npy1r^{rfb} mutant mice), induces a significant slowdown in spatial learning, which is associated with a robust intensification of PNN expression and an increase in the number of c-Fos expressing cells in the cornus ammonis 1 (CA1) of the dorsal hippocampus. Importantly, the enzymatic digestion of PNNs in CA1 normalizes c-Fos activity and completely rescues learning abilities of Npy1r^{rfb} mice. These data highlight a previously unknown functional link between NPY-Y1R transmission and PNNs, which may play a role in the control of dorsal hippocampal excitability and related cognitive functions.

Keywords: Neuropeptide Y, perineuronal nets, chondroitinase, brain plasticity, c-Fos, hippocampus

Abbreviations: CA1, cornus ammonis 1; CA2, cornus ammonis 2; CA3, cornus ammonis 3; CamKII, calcium/calmodulin dependent protein kinase II; ChABC, chondroitinase ABC; Cre, cre recombinase; CSPG, chondroitin sulfate proteoglycans; DAPI, 4′,6-diamidino-2-phenylindole; DG, dentate gyrus; EE, enriched environment; GABA, gamma-aminobutyric acid; MWM, Morris water maze; NeuN, neuronal nuclear protein; NPY, neuropeptide Y; *Npy1r*, gene encoding the Y1 receptor for NPY; OF, open field; PBS, phosphate buffer saline; PNN, perineuronal net; PV, parvalbumin; s.o., stratum oriens; s.p., stratum pyramidalis; s.r. stratum radiatum; WFA, *Wisteria floribunda agglutinin*; Y1R, Y1 receptor.

1. Introduction

Perineuronal nets (PNNs) are lattice-like aggregates of extracellular matrix molecules, including chondroitin sulfate proteoglycans (CSPGs), which form around the soma and dendrites of central nervous system (CNS) neurons during postnatal development in an activity-dependent manner, contributing to the closure of developmental critical periods of heightened plasticity (Fawcett et al., 2019).

PNNs surround both excitatory and inhibitory neurons. In the cortex, they are found preferentially around fast-spiking parvalbumin (PV)-positive gamma-aminobutyric acid (GABA)ergic neurons, which are critically involved in the regulation of synchronous oscillatory output of pyramidal neurons (Lensjø et al., 2017). Experimental manipulations that interfere with PNNs, such as enzymatic digestion of CSPGs by chondroitinase ABC (ChABC), manipulation of PNN components or exposure to enriched environment (EE), restore plastic capabilities typical of critical periods, induce axon sprouting and enhance learning capabilities and cognitive flexibility (Carulli et al., 2010; Foscarin et al., 2011; Geissler et al., 2013; Gogolla et al., 2009; Happel et al., 2014; Hirono et al., 2018; Pizzorusso et al., 2002; Carulli et al., 2020). Interestingly, depending on the genotype, EE can drive opposite effects on numbers of PV^+/PNN^+ cells, thereby favoring the establishment of an "optimal" range for PV^+/PNN^+ cell numbers in the hippocampus, which allows memory enhancement (Cattaud et al., 2018).

Nonetheless, PNNs are also shown to contribute to memory formation and consolidation (Banerjee et al., 2017; Blacktop et al., 2017; Hylin et al., 2013; Romberg et al., 2013; Slaker et al., 2015; Thompson et al., 2018; Xue et al., 2014).

Neuropeptide Y (NPY) is a widely distributed peptide in the CNS, involved in the regulation of a plethora of many different physiological functions such as anxiety, stress response, energy balance and cognition (Enman et al., 2015; Gøtzsche and Woldbye, 2016; Loh et al., 2015; Reichmann and Holzer, 2016). In the brain, NPY interacts with a family of G protein–coupled receptors that includes the Y1 (Y1R), Y5 (Y5R), and Y2 receptors, the last one considered to function mainly as a presynaptic receptor (Eva et al., 2006).

NPY plays both inhibitory and stimulatory effects in learning and memory, depending on the type of memory, brain region and receptor subtype. There is compelling evidence that the NPY-Y1R signal differently modulates learning and memory processes and synaptic transmission (Gøtzsche and Woldbye, 2016). Stimulation of Y1Rs, which produces a potent anxiolytic effect, suppresses fear learning in cued and contextual conditioning in several brain areas, including amygdala and hippocampus (Gutman et al., 2008; Hörmer et al., 2018; Lach and de Lima, 2013). Other studies have investigated a potential role for Y1R in spatial learning and memory. Pharmacological experiments have shown that intracerebroventricular administration of NPY or Y1R agonists prevents spatial memory deficits in rats with an Alzheimer's disease-like phenotype (Rangani et al., 2012) and reverts memory deficit induced by N-methyl-D-aspartate (NMDA) receptor channel blockers (Eaton et al., 2007). Spatial learning in the Morris water maze (MWM) increases NPY mRNA expression levels in the dentate gyrus (DG) (Hadad-Ophir et al., 2014), and exposure to EE impairs spatial memory and hippocampal synaptic plasticity in NPY null but not in wild type mice, suggesting that the NPY system could be a target for “enviromimetics” and that the NPY deletion reverses the beneficial e□ects of EE into a negative experience (Reichmann et al., 2016). Interestingly, Y1R signaling is critical for the control of principal cells intracellular calcium homeostasis in the hippocampus (Gøtzsche and Woldbye, 2016; Hamilton et al., 2010).

In this study, we investigated whether NPY-Y1R signaling may affect learning and memory through modulation of PNNs. To this aim we employed conditional knockout mice in which the gene encoding the Y1R for NPY (*Npy1r*) was specifically inactivated in forebrain principal neurons starting from juvenile age (Npy1r^{rfb} mice) (Bertocchi et al., 2011). Here we demonstrate that the conditional inactivation of *Npy1r* gene in limbic excitatory neurons impairs spatial learning, increases the number of cells expressing c-Fos, an established marker for neural activity (Kovacs, 2008; Marrone et al., 2008), and enhances the intensity of PNN coating around the soma of CA1 neurons of the dorsal hippocampus. Moreover, ChABC-mediated disruption of the PNNs in the CA1 reestablishes neuronal activity homeostasis in Npy1r^{rfb} mice, thereby restoring learning performance. Together, these data suggest a previously unknown cooperative role of NPY-Y1R transmission and PNNs, two key regulators of neuronal plasticity, in maintaining the appropriately

tuned activity and, possibly, the optimal excitation-to-inhibition balance for hippocampal-dependent learning.

2. Material and Methods

2.1 Mice

The methods for gene targeting at the Npy1r gene loci and generation of Npy1r^{rfb} mice (C57BL6/129/SvJ-derived strain) were performed as described in detail previously (Bertocchi et al., 2011). Briefly, the forebrain specific genetic deletion in mice of the entire *Npy1r* coding region was achieved using compound genetically-modified mice encoding (i) the homozygous floxed Npy1$^{tm1.2Ceva}$ gene (MGI: 5307899; named herein Npy1r$^{fl/fl}$) combined with heterozygous transgenes of mouse strains carrying (ii) the forebrain specifically expressed transgene of tTA (Tg$^{(Camk2a\text{-}tTA)1Mmay/J}$; Jackson lab: Strain 003010; named herein Tg$^{CamKIIa\text{-}tTA}$) and (iii) the tTA dependent Cre transgene (Tg$^{(tetO\text{-}cre)LC1Bjd}$; MGI:2448952; named herein Tg$^{(tetO\text{-}cre)LC1}$) (for further details see Bertocchi et al., 2011). Using this combination of the tTA (Tg$^{CamKIIa\text{-}tTA}$) and Cre (Tg$^{(tetO\text{-}cre)LC1}$) regulated gene expression system, we achieved the deletion of *Npy1r* gene specifically in excitatory neurons of the limbic system, starting from juvenile stages. In male mice, conditional deletion of *Npy1r* gene was observed in the dentate gyrus, CA1 and CA3 subregions of the hippocampus and in the cerebral cortex (Bertocchi et al., 2011; 2020). Littermates comprising Npy1$^{rfl/fl}$/Tg$^{CamKIIa\text{-}tTA}$, Npy1$^{rfl/fl/Tg(tetO\text{-}cre)LC1}$, and Npy1r$^{fl/fl}$ genotypes were used as controls (named herein Npy1r^{2lox} controls). *Tg$^{CamKIIa\text{-}tTA}$* mice were backcrossed for more than 10 generations to C57Bl/6N mice while the other mouse lines were bred in their colony; the coat color of the investigated mice was still mixed ‘mainly black’ indicating that the genetic background of the investigated population is very heterogeneous, which suggests that the observed phenotype is independent from the genetic background (Silva et al., 1997). Genotyping was performed as described previously (Bertocchi et al., 2011; Shimshek et al., 2006).

Five months old male mice were caged in groups of 2–6, in a temperature- (22±1 °C) and humidity- (50±10%) controlled housing room on a 12-h light/dark cycle (8:00 AM–8:00 PM) and had ad libitum access to food and water.

The current study was performed using male mice since female mutants did not show differences in learning and memory functions and in cognitive performance (Bertocchi et al., 2020; Oberto et al., in preparation).

All experiments were conducted in accordance with the European Community Council Directive of 24 November 1986 (86/EEC) and approved by the University of Turin Ethical Committee for animal research and by the Italian Ministry of Health *(license no. 139/14).*

2.2 Behavioral analysis

Before the behavioral experiments (carried out between P70 and P90), mice were familiarized to the experimenter who was blind to the genotype, with repeated weighing and handling. All tests were performed between 9 a.m. and 12 p.m. on male littermate mice from different cohorts. On test day, mice were transported to a dimly illuminated (2 x 40 W, indirect) testing room, adjacent to the animal housing area, and left undisturbed for at least 30 min before testing. At the end of each trial, the apparatus was accurately cleaned up with ethanol 2% and water. Data was recorded automatically from the digitized image by using video-tracking (Ethovision XT video track system; Noldus Information Technology, Wageningen, The Netherlands).

2.2.1 Open field test

Open field (OF), to test anxiety and locomotor activity, was performed between P70 and P75 from 8-10 a.m. Mice were placed in a PVC arena (50 x 50 cm) which was divided into a central (25 x 25 cm) and a peripheral zone. The mouse was placed in the corner of the open field and was allowed to explore the arena for 10 min. Distance travelled and time spent in the central area were recorded. Locomotor activity was assessed by measuring the total path-length travelled by the mouse in the arena.

2.2.2 *Morris water maze*

The acquisition phase and the probe trial (day 1-5) were performed as previously described (Longo et al., 2014; 2018). Briefly, an escape platform was placed in the center of one quadrant (target

zone) of a circular pool and it was hidden 1 cm beneath the water surface. The water (24 ± 1 C) was made opaque with powdered milk. The acquisition phase consisted of four trials per day with a 20 min inter-trial interval for four consecutive days (day 1-4). Four points equally spaced along the circumference of the pool (North, South, East, West) served as the starting position, which was randomized across the four trials each day. Mice were given 90 s to find the hidden platform. If a mouse did not reach the platform within 90 s, it was gently guided to the platform, where it had to remain for 30 s. The escape latencies, percentage of distance travelled and of time spent in each quadrant were recorded. On day 5 (probe trial) the platform was removed, and mice were allowed to swim freely for 90 s in the maze. The percentage of distance travelled and of time spent in each quadrant and the swim speed were calculated.

2.2.3 Barnes maze

A different set of mice was tested in a 15-trials version of the Barnes maze (Attar et al., 2013). The maze consisted of a white cleanable disk-shaped arena (140 cm diameter) with 36 holes of 5 cm diameter on the border and with an escape black box positioned immediately below the escape hole to be easily accessible by the mice. In the test room, brightly illuminated and kept asymmetric by the use of visual cues, a loud white noise (about 70 dB) was played by an external operator through PC speakers. In the habituation phase (trial 1) the mouse was placed underneath a wired cylinder and gently guided to the escape hole allowing the mouse to spontaneously enter. During the same day two more trials were conducted, in which the mice were left free to explore the arena and enter the box. During the acquisition phase (day 2-4), four trials a day were run; the maximum duration of each trial was set to 2 minutes and the intertrial interval was about 15 minutes. The escape latencies, the time spent in each quadrant and the total walked distance were recorded. On day 6 (probe trial) the escape box was removed, and mice were allowed to freely explore the maze for maximum 2 minutes. The time spent in each quadrant and the total walked distance were calculated.

2.3 Intra-hippocampal stereotaxic ChABC injection

Gas anesthesia was induced in a chamber in which 3% isoflurane was dissolved in a mixture of N_2O / O_2 (30:70). Randomized mice were then fixed on a stereotaxic apparatus and the anesthesia maintained through a nose mask with 1.5% isoflurane in the same mixture. ChABC (25 U/ml, AMSBIO, Abingdon, UK) was pressure-injected bilaterally (0.5 µl/side) in the CA1 (Bregma -2.2 mm; lateral 1.5 mm; depth 1.6 mm) by a glass capillary connected to a PV800 Pneumatic Picopump (WPI, New Haven, CT). Each injection was delivered in about 5 min, afterwards the capillary was left for two minutes *in situ* to allow solution diffusion. Finally, the mice were sutured and received normal post-operative care and allowed to recover and rest for 3 days. On the fourth day they were subjected to the MWM.

2.4 Immunohistochemistry

Mice were transcardially perfused with 4% formaldehyde in phosphate buffer saline (PBS) and the removed brain cryoprotected and frozen at -80°C. For c-Fos staining, mice were perfused 90 minutes after the last Barnes test session, time during which they were maintained undisturbed in their own cages. Coronal 25 µm-thick brain sections were obtained with a cryostat (Leica Microsystem, Milano, Italy) and series corresponding to the dorsal hippocampus were then blocked with 10% normal goat serum for 1 h at room temperature before the incubation with primary antibody. Detection of PNNs was performed by using biotinylated *Wisteria floribunda agglutinin* (WFA) (Sigma-Aldrich, Milano, Italy) 1:200 for two hours at room temperature or rabbit anti-aggrecan antibody (Synaptic System, Goettingen, Germany) 1:1500 overnight at 4°C. For double, triple or quadruple staining mouse or rabbit anti-parvalbumin (Swant, Bellinzona, Switzerland) 1:1500, rabbit anti c-Fos (Cell Signaling) 1:1000 and mouse anti-neuronal nuclear protein (NeuN, Merck Millipore, Milano, Italy) 1:500 or 4′,6-diamidino-2-phenylindole (DAPI) (Merk Millipore, Milano, Italy) 1:10000 were combined with WFA or anti-aggrecan antibody and incubated overnight at 4°C. To reveal biotinylated WFA, Texas Red streptavidin (Jackson Immuno Research, West Grove, USA) 1:500 was used for 1 hr at room temperature, whereas for the detection of the other markers, anti-rabbit or anti-mouse Alexa Fluor 488 (Life Technologies, Milano, Italy) 1:500 and

anti-rabbit or anti-mouse Alexa Fluor 647 (Life Technologies, Milano, Italy) 1:400 were incubated for 1 hr at room temperature. All antibodies were dissolved in 1x PBS/0.2% Triton X-100.

2.5 Image Analysis

Confocal images were acquired with a Nikon Eclipse-C1 confocal microscope (Nikon Instruments, Firenze, Italy) under a 40x objective with 1 N/A at 100 Hz scan speed, format 1024x1024 pixels, resolution 0.31 µm/pixel, Zstep size 1µm and a color depth of 8 bits per channel, through the EZ-C1 software (Nikon Instruments, Firenze, Italy). Laser intensity, gain and offset were maintained constant in each analysis and the intensity of the signal never reached saturation levels. Quantitative and morphometric evaluations on samples were made by investigators blinded to genotype or treatment using the software ImageJ (http://rsbweb.nih.gov/ij/index.html) or Neurolucida (Bioscience, Williston, USA, version 10.30.1) which was connected to an E-800 Nikon microscope via a color CCD camera to trace dendrites live, under a 20x objective with 0.50 N/A, 0.36 µm/pixel resolution, to subsequently import data to Neurolucida Explorer (MBF Bioscience, Williston, USA) for the Sholl analysis. Exposure time, gain and offset were, also in this case, kept constant during the whole study. Adobe Photoshop (Adobe Systems, San Jose, CA) was used to assemble the final figures and to adjust image contrast on the entire figure, after all the analyses were completed.

2.5.1 PNN fluorescence intensity

PNN expression was evaluated by quantifying the staining intensity of WFA and aggrecan around individual neurons of the dorsal hippocampus. WFA is a lectin that binds glycosaminoglycan chains of CSPGs, and is commonly used as a general marker for PNNs (Härtig et al., 1992; Lapray et al., 2012). Aggrecan is an abundant CSPG in the PNN, which is crucial for PNN formation and maintenance (Rowlands et al., 2018). Our analysis was focused on the CA1, CA3 and dentate gyrus (DG) hippocampal subregions, whereas the CA2 area was excluded because the border of individual PNN structures herein was difficult to identify (Horii-Hayashi et al., 2015).

For the analysis of WFA or aggrecan staining intensity, confocal images of sections of the dorsal hippocampus (1.50 to 2.50 mm caudal to Bregma) were acquired under a 40x objective. Twelve to 15 µm stacks were assembled and analyzed with ImageJ. Four sections/mouse were analyzed, bilaterally. To measure PNN fluorescence intensity we chose the step (1 um thick) in the stack in which the net reached the maximum width that usually corresponds to the brightest signal. The area was selected by drawing a ring along the borders of the WFA- or aggrecan-positive net around the neuronal soma, and the mean brightness intensity (range 0–255) was measured. The background signal taken from two unstained areas in the surrounding region was subtracted from the PNN fluorescence intensity. Each PNN positive neuron was then assigned to one of three categories of staining intensity, ranging from the lowest to the highest detected value of WFA or aggrecan: weak = 0–33%, medium = 34–66%, strong = 67–100% of maximum staining intensity (Foscarin et al., 2011).

2.5.2 PNN colocalization

To measure the percentage of colocalization of WFA with PV, c-Fos and NeuN or DAPI, sections were acquired as described above and the analysis was conducted throughout the stack by calculating the percentage of neurons with co-labeling of markers.

2.5.3 PNN complexity

To measure the extension of PNN coating along dendrites, we performed Sholl analysis following dendrites tracing using Neurolucida 10.30.1. In brief a series of 10 µm spaced concentric rings were centered on the soma and the number of dendritic intersections with the rings was counted as a quantitative assessment of complexity. The sum of the length of dendritic segments in between two consecutive rings was also calculated.

2.5.4 c-Fos analysis and colocalization

To measure the percentage of colocalization of c-Fos with PV, NeuN or DAPI, sections were acquired at the confocal microscope as described above. Two different CA1 AOI of 4 different

sections (8 areas in total) for each mouse (n=4-5) were analyzed, by an observer blinded to genotype and treatment, throughout the 12 to 15 µm stacks with ImageJ, and the percentage of c-Fos positive cells within these areas was calculated and averaged.

2.6 Statistical Analysis

Acquisition phase and probe trials in the MWM and Barnes maze and Sholl analysis were analysed by two or three-way ANOVA for repeated measures followed by Newman Keuls post-hoc test for multiple comparisons, when indicated. We used the χ^2-test to compare the distribution of frequencies with respect to staining intensity categories. Graphs and data are represented as mean ± standard error of the mean (SEM) unless otherwise specified and the level of statistical significance was set at $p < 0.05$. Data were analyzed using the STATISTICA software (StatSoft, Inc).

3. Results

3.1 Npy1r^{rfb} mice display deficits in spatial learning

To elucidate the role of NPY-Y1R signaling in learning and memory, we compared the performance of Npy1r^{rfb} conditional mutants and control mice (Npy1r^{2lox}) in the MWM and the Barnes maze tests.

In the MWM, male Npy1r^{rfb} mice show a significantly slower decline of latency to find the hidden platform over 4 days of training, compared to their control littermates (two-way ANOVA for repeated measures reveals a significant effect of genotype [$F(1,22)= 4.66$, $p=0.042$] and of days [$F(3,66)= 47.2$, $p<0.001$] and a not significant effect of genotype x days interaction [$F(3,66)= 0.36$, $p=0.78$]; n=12 from 8 litters, Fig. 1A and E). In the Barnes maze, male Npy1r^{rfb} mice show a longer latency in finding the target hole and entering the escape cage over 15 learning trials (two-way ANOVA for repeated measures reveals a significant effect of genotype [$F(1,7)= 6.12$, $p=0.042$] and of days [$F(3,21)= 19.8$, $p<0.001$] and a not significant effect of genotype x days interaction [$F(3,21)= 2.42$, $p=0.095$]; n=4-5 from 2-4 litters, Fig. 1B).

In the probe trial of both tests, mutant mice and their control littermates display a similar preference for the target zone, since no significant differences in the percentage of time spent in it were observed between genotypes (two-way ANOVA for repeated measures reveals a significant effect of quadrants [MWM: $F(3,48)= 13.9$, $p<0.001$; Barnes maze: $F(3,21)= 39.7$, $p<0.001$] but a not significant effect of genotype [MWM: $F(1,16)= 70.19$, $p=0.67$; Barnes maze: $F(1,7)= 0.81$, $p=0.40$] and of genotype x quadrant interaction [MWM: $F(3,48)= 0.74$, $p=0.53$; Barnes maze: $F(3,21)= 1.74$; $p=0.19$], Fig. 1C and D).

No significant difference in swim ability was observed between Npy1r^{rfb} *and* Npy1r^{2lox} mice (Suppl. Fig. 1A). Npy1r^{rfb} mice also showed no differences in the total distance travelled in the OF compared to Npy1r^{2lox} mice, suggesting that the conditional inactivation of *Npy1r* gene in limbic excitatory neurons does not affect locomotor activity as previously reported (Bertocchi et al., 2011, Suppl. Fig. 1B).

3.2 PNNs are more intensely stained and more extended along projections in the CA1 of Npy1r^{rfb} mice

To examine whether the deficit in learning observed in Npy1r^{rfb} mice was associated with differences in PNN expression in the dorsal hippocampus, we performed a staining with WFA. The percentage of PV^{+} and PV^{-} neurons enwrapped by WFA-positive PNNs in the CA1, CA3 and DG hippocampal subregions is comparable between genotypes (Table 1).

As shown in Fig 2A and C, the number of neurons surrounded by strongly stained WFA+ PNNs is significantly higher in the CA1 (in both the stratum pyramidalis, s.p., and the stratum oriens, s.o.) of Npy1r^{rfb} mice compared to their control littermates (s.p.: $\chi^2(2)= 35.5$, $p<0.001$; s.o.: $\chi^2(2)= 8.18$, $p< 0.05$; n=9-11 from 5-6 litters). To test the hypothesis that not only the sugar chains but also the core proteins of CSPG are altered, we used an antibody against aggrecan, an abundant CSPG in the PNNs. We found that Npy1r^{rfb} mice also bear more neurons enwrapped by intense aggrecan-stained PNNs in the CA1 in the s.p. when compared to control mice (s.p.: $\chi^2(2)= 16.4$, $p<0.001$; n=9-11 from 5-6 litters) (Fig. 2B, D).

No significant difference in WFA or aggrecan staining intensity is detected in the CA3 region and in the dentate gyrus between Npy1r^{2lox} and Npy1r^{rfb} mice (Suppl. Fig. 2).

Since no significant differences in PNN intensity were observed in the CA3 subregion and in the dentate gyrus, we then restricted further analyses to the CA1 subregion. First, we analyzed the intensity of PNN around CA1 PV$^+$ GABAergic neurons, which represent the vast majority of PNN wrapped neurons both in control and mutant mice (Table 1). As shown in Fig. 3A and C, the intensity of WFA signal around PV$^+$ neurons in the s.p. and s.o. of the CA1 is significantly stronger in Npy1r^{rfb} mice than in their control littermates (s.p.: $\chi^2(2) = 18.2$, $p<0.001$; s.o.: $\chi^2(2) = 9.30$, $p=0.01$; n=9-11 from 5-6 litters). Npy1r^{rfb} mice also display a more intense staining for PNNs around the PV negative neurons in the s.p. of the CA1 (s.p.: $\chi^2(2) = 14.0$, $p<0.001$; n=9-11 from 5-6 litters) (Fig. 3B, D).

To assess whether the observed increased staining intensity is also accompanied by an increased extension of PNN coating along dendrites, we analyzed the PNN coating complexity by tracing WFA signal on dendrites of neurons whose soma lie in the s.p. of the CA1. Sholl analysis (Fig. 4A) shows that the number of intersections are significantly higher in Npy1r^{rfb} mice at 32, 72, 82 and 92 µm from the soma, compared to Npy1r^{2lox} mice (ring intersections: two-way ANOVA for repeated measures reveals a significant effect of genotype [$F(1,17)=6.18$, $p=0.024$], distance from soma [$F(19,323)=274$, $p<0.001$] and genotype x distance from soma interaction [$F(19,323)=2.74$, $p<0.001$; n=9-10 from 5-6 litters], Fig. 4B, left). Moreover, the length of WFA-covered dendrites, included in two consecutive rings, is overall higher for conditional mutants, in particular at 42, 62, 72, 82, 92, 102 and 112 µm from the soma (length: two-way ANOVA for repeated measures reveals a significant effect of genotype [$F(1,17)=6.34$, $p=0.02$], distance from soma [$F(20,340)=300$, $p<0.001$] and genotype x branching order interaction [$F(20,340)=2.93$, $p<0.001$]; n=9-10 from 5-6 litters, Fig. 4B, right). Since neurons in the hippocampus and its subregions are anatomically and functionally strongly polarized, we also ran the Sholl analysis separately for the s.o. and the stratum radiatum (s.r.) of the CA1 (Fig. 4C and D). We found that WFA coating is significantly more branched and more extended in length in the s.o. of Npy1r^{rfb} mice (ring intersections: two-way ANOVA for repeated measures reveals a significant effect of genotype

[F(1,17)=12.26, p=0.003], distance from soma [F(19,323)=257, p<0.001] and genotype x distance from soma interaction [F(19,323)=5.11, p<0.001]; length: two-way ANOVA for repeated measures reveals a significant effect of genotype [F(1,17)=9.01, p=0.008], distance from soma [F(19,323)=285, p<0.001] and genotype x distance from soma interaction [F(19,323)=3.96, p<0.001]; n=9-10 from 5-6 litters, Fig 4C), while, in the s.r., both genotypes show comparable length and intersections of WFA positive coating (Fig 4D).

3.3 Intrahippocampal ChABC injection rescues spatial learning deficits of Npy1r^{rfb} mice.

To test whether the increased PNN intensity plays a role in the learning deficits of Npy1r^{rfb} mice, PNNs of the CA1 have been digested, in both control and mutant mice, by means of bilateral injection of ChABC, which is known to digest CSPGs already 24 hours after the treatment (Crespo et al., 2007). Three days after injection of ChABC or saline, 2 different cohorts of mice have been subjected to MWM or Barnes maze test, respectively (Fig 5A). Histochemical staining with WFA revealed that the intensity of PNNs is still significantly reduced in the CA1 eight days after the injection (namely at the end of the spatial memory test), in both conditional mutants and their control littermates (Fig. 5B).

Fig 5C illustrates that removal of PNNs in the CA1 does not influence spatial learning of Npy1r^{2lox} control mice in the acquisition phase of MWM. Conversely, ChABC treated Npy1r^{rfb} mice display a significant lower latency to find the hidden platform over the days of training, compared to saline treated Npy1r^{rfb} mice (two-way ANOVA for repeated measures reveals a significant effect of days [F(3,219)=190, p<0.001] and genotype [F(1,73)=7.55, p=0.008] and of genotype x treatment [F(1,73)=6.37, p=0.014] and genotype x treatment x days [F(3,219)=3.66, p=0.013] interactions, but not significant effect of genotype x days interaction [F(3,219)=0,55, p=0,65]; n=13-23 from 19 litters, Fig 5C). These results were replicated in the Barnes maze test with a different cohort of mice. Consistently, the removal of PNNs by ChABC treatment restores the learning abilities of Npy1r^{rfb} mice (Fig. 5D). Interestingly, ChABC treatment transiently reduces the escape latency of Npy1r^{2lox} mice on the second day of training (two-way ANOVA for repeated measures reveals a significant effect of genotype [F(1,14)=14.14, p=0.002], treatment [F(1,14)=9.46, p=0.008], days

[F(3,42)=44.89, p<0.001] and of genotype x days [F(3,42)=3.50, p=0.023] and genotype x treatment x days [F(3,42)=3.52, p=0.023] interactions; n=4-5 from 5 litters, Fig. 5D). No significant differences in memory performance are observed among groups in the probe day trial on day five in both tests (MWM: three-way ANOVA for repeated measure reveals a significant effect of quadrants [F(3,219)= 55.4, p<0.001] and of genotype x quadrant interaction [F(3,219)= 2.99, p=0.032]; Barnes maze: three-way ANOVA for repeated measure reveals a significant effect of quadrants [F(3,42)= 10.9, p<0.001] but no significant effect of genotype [F(3,42)= 10.9, p<0.001] and genotype x quadrant interaction, Fig. 5 E-F).

3.4 Npy1r^{rfb} mice display increased neuronal activity in the CA1

To give a possible mechanistic explanation to our findings, we analyzed c-Fos expression in the CA1 of ChABC- and saline-treated mice having performed the Barnes maze test. Saline-injected Npy1r^{rfb} mice showed a significant increase in the number of c-Fos expressing cells in the stratum pyramidalis of CA1 (Fig 6 and Table 2). Intriguingly, this overactivation is reverted by ChABC treatment (two-way ANOVA reveals a significant effect of genotype x treatment interaction [F(1,13)=10, p=0.007]; n=4-5 from 5 litters, Fig 6B). As shown in Fig 6, the inactivation of *Npy1r* gene increases c-Fos expression in PV-negative cells, which represent the majority (~90%) of the total number of c-Fos positive cells (percentage of c-Fos$^+$/DAPI: two-way ANOVA reveals a significant effect of genotype x treatment interaction [F(1,13)=10, p=0.007]; percentage of PV$^+$c-Fos$^+$/c-Fos$^+$: two-way ANOVA reveals a significant effect of treatment [F(1,16)=5.83, p=0.028], Table 2).

4. Discussion

Emerging evidence shows that PNNs are critically involved in learning and memory processes and are affected in several neurodevelopmental disorders characterized by cognitive impairment (Pantazopoulos and Berretta, 2016). Accordingly, their number, integrity and appearance vary among brain regions as a function of normal physiology and network architecture and also in pathologies (Fawcett et al., 2019; Kwok et al., 2011; Bozzelli et al., 2018).

Here we investigated learning and memory functions in Npy1r^{rfb} conditional mice that carry the inactivation of *Npy1r* gene selectively in excitatory forebrain neurons of the limbic system, particularly in the hippocampal formation, of adolescent mice (Bertocchi et al., 2011; Bertocchi et al., 2020). Npy1r^{rfb} male mice show a significant slowdown of the spatial learning curve in the MWM and Barnes maze tests, indicating that the NPY-Y1R signal in the dorsal hippocampus plays a crucial role in learning ability.

In parallel, Npy1r^{rfb} male mice show an increase of c-Fos expression in putative pyramidal neurons of the CA1 subfield of the dorsal hippocampus and a robust intensification of PNNs in the same hippocampal region, around both PV^{+} and PV^{-} neurons. The increase in c-Fos staining observed in the CA1 of Npy1r^{rfb} mice is independent of their activity state since conditional mutant mice didn't show any difference in locomotor activity in the MWM and in the OF arena. Most importantly, after injecting the ChABC enzyme specifically into the CA1 of mutant mice, we obtained a complete rescue of learning abilities of Npy1r^{rfb} male mice and c-Fos expression normalization. Our data are in line with previous studies showing that PNN digestion in the hippocampus enhances inhibition. Namely, an increase in the frequency of spontaneous inhibitory postsynaptic currents is observed in CA1 pyramidal neurons, which is accompanied by LTP deficits and impaired fear memory consolidation (Shi et al. 2019). Furthermore, injection of ChABC in the hippocampus of rats with chronic depressive-like state, which are characterized by increased number of PNNs surrounding PV-expressing interneurons, decreased frequency of inhibitory postsynaptic currents in CA1 pyramidal neurons and impaired short-term object location memory, restores the number of PNNs, hippocampal inhibitory tone and memory performance (Riga et al., 2017).

Modulation of the inhibitory status appears to be essential in different processes of neuronal plasticity related to learning and memory (Froemke and Schreiner, 2015; Letzkus et al., 2015). The dorsal part of the hippocampus is organized in a tri-synaptic pathway (Amaral and Witter, 1989) and depends on glutamate release, while GABA and several neuromodulators, which are co-released from inhibitory interneurons, provide fine-tuning (Hörmer et al., 2018). Neuromodulators can affect the impact of sensory experience on critical periods as well as on adult plasticity by regulating neuronal excitability, improving signal to noise ratio, and controlling the propagation of

activity (Seol et al., 2007). NPY is expressed in GABAergic neurons, including the PV positive subclass, and acts as a homeostatic regulator of cortical and hippocampal excitatory neurotransmission (Oberto et al., 2001; Hei et al., 2018; Karagiannis et al., 2009). Y1Rs, mainly located post-synaptically, exert potent anti-excitatory actions by decreasing glutamate release in several brain regions, including the hippocampus (Stanić et al., 2011; Vollmer et al., 2016). Thus, the decrease of the inhibitory NPYergic tone in principal neurons of the CA1 of Npy1r^{rfb} mice, where the reduction of the receptor expression is particularly significant (Bertocchi et al., 2011), might increase excitability of pyramidal neurons and, in turn, of c-Fos neuronal activity, leading to an unbalanced excitation-to-inhibition ratio toward hyperexcitability. This hypothesis is in line with recent studies showing that repetitive transcranial magnetic stimulation (iTBS) promotes learning (Dayan et al., 2013; Ridding and Ziemann, 2010) potentially via transient changes in the excitation-inhibition balance (Lenz et al., 2016; Ziemann and Siebner, 2008). The changes in cortical excitability following iTBS seem to be in part related to the dampening of glutamate release via increased NPY signaling. This results in the decrease of the ratio of high-(mature) to low-(immature) expressing PV$^+$ fast spiking neurons and of their excitatory inputs (Jazmati et al., 2018). The maturation of PV$^+$ cells is accompanied by the condensation of PNNs around their soma and dendrites (Sigal et al., 2019) suggesting that NPY signaling might act as a negative modulator of PV$^+$ neurons and PNN maturation.

We suggest that the increased excitatory drive onto CA1 cells of the dorsal hippocampus of Npy1r^{rfb} male mice might account for the augmented amount of PNNs that, in turn, could explain the learning deficits. Interestingly, Sholl analysis demonstrates an increased thickness of PNN around the CA1 pyramidal cell bodies and their proximal dendrites in the stratum oriens, both of which under the influence of the GABAergic interneuron inhibitory tone. The long-lasting actions of NPY, whose release requires intense stimulation, might modulate and alter the threshold for plasticity more effectively than GABA (Reibel et al., 2000).

In recent years, several studies have documented that PNNs limit learning abilities and consolidate or maintain memories over time (Romberg et al., 2013; Happel et al., 2014; Banerjee et al., 2017, Thompson et al., 2018; Carulli et al., 2020).

The CA1 is a brain region where pyramidal place cells dynamically fire to encode space according to environmental cues (O'Keefe and Dostrovsky, 1971). PNNs intensification in the CA1 of Npy1r^{rfb} mutant mice may be due to a reduction of the dynamism in excitation of place cells, which is important to build an appropriate cognitive map during learning, and in turn, render navigation efficient. Accordingly, EE, which decreases PNNs expression in several brain regions (Carstens et al., 2016; Foscarin et al., 2011; Sale et al., 2007), enhances spatial learning via a mechanism that was postulated to affect place cells, which become more flexible to remap following environmental changes (Ohline et al., 2018).

Interestingly, we have shown that ChABC treatment decreases the escape latency of Npy1r^{2lox} control mice in the Barnes maze test but not in the MWM. By forcing mice to swim, the MWM has a more stressful component compared to the Barnes maze that can affect learning and memory performance (Harrison et al., 2009). Since mice and rats are more physiologically adapted to dry land tasks, the Barnes maze may better elucidate certain learning/navigation behaviors (Whishaw and Tomie, 1996). Accordingly, the learning impairment of Npy1r^{rfb} mice, which display anxious-like behaviour compared to their control littermates (Bertocchi et al., 2011), is more pronounced in the Barnes than in the MWM test. On the other hand, the observation that ChABC treatment ameliorates learning performance in control mice on the second day of training in the Barnes test suggests that other pathways different from the NPY-Y1R transmission may be involved in the PNN modulation of learning abilities. However, our data indicate that the magnitude of the effect of ChABC on Npy1r^{rfb} conditional mutant mice is significantly higher than that observed in control mice, as indicated by statistical analysis (ANOVA: genotype x treatment x days [$F(3,42)=3.52$, $p=0.023$). There is a constant decrease of escape latency in Npy1r^{rfb} mice, observed in particular on the 3rd and 4th day of training (Fig. 5). This indicates a different effect of ChABC treatment on control and Npy1r^{rfb} mice that, together with the observation that in the MWM ChABC increases learning ability in conditional knockout but not control mice, support the hypothesis that NPY-Y1R transmission facilitates learning by modulating CA1 PNNs and suggest the existence of a close link between Y1R and PNNs.

In the present study, we did not find differences between mouse groups in the probe trial of MWM and Barnes tests, and PNN removal does not affect memory performance in both groups, suggesting that PNNs are not involved in spatial reference memory. In addition, as discussed above, we observed that PNN digestion has a lower impact on spatial learning performance of control mice when compared to Npy1r^{rfb} mice. Because PNNs are strongly implicated in the long term retention process of several types of memories (Gogolla et al. 2009; Thompson et al. 2018; Carulli et al. 2020), we cannot exclude that hippocampal PNNs may be involved in the storage and/or retrieval of remote memories.

Finally, we demonstrated that ChABC treatment fails to affect c-Fos expression in Npy1r^{2lox} mice, suggesting that the increase of structural and synaptic plasticity, induced by PNN digestion, restores the phenotype only where the equilibrium is altered, hence in Npy1r^{rfb} mice and not in controls. In general, compared to other brain regions such as sensory cortices, the dorsal hippocampus has lower expression of PNNs, which may reflect its need of high level of plasticity even in adulthood (Yamada and Jinno, 2013). In accordance, the variable inter- and intra-regional expression patterns of PNNs in the brain may reflect different levels of plasticity and wiring of neuronal networks (Lensjø et al., 2017; Bozzelli et al., 2018). Indeed, it has been previously suggested that PNNs expression in the hippocampus, and in particular the CA1 subfield, is kept under a certain threshold to allow retaining the plasticity necessary to learn new information (Hylin et al., 2013).

In conclusion, here we provide novel evidence that the NPY-Y1R transmission facilitates learning possibly by modulating CA1 PNNs and c-Fos expression and, thereby, hippocampal plasticity and activity. Further studies will be needed to identify the precise molecular mechanisms underlying these processes, which may lead to the development of new therapeutic strategies for the treatment of a number of neuropathologies associated with altered excitation/inhibition balance and PNN expression.

Funding: This work was supported by the Italian Ministry of University and Research (PRIN 2008PLKP3E_003), Neuroscience program-Compagnia di San Paolo, Torino

(S1315_RIC14_L2_EVC_01) and Fondazione CRT, Torino to CE; Fondazione Veronesi fellowship 2014 to PM.

References

Amaral, D. G., Witter, M. P., 1989. The three-dimensional organization of the hippocampal formation: a review of anatomical data. Neuroscience 31, 571-591.
Attar, A., Liu, T., Chan, W.-T. C., Hayes, J., Nejad, M., Lei, K., Bitan, G., 2013. A shortened Barnes maze protocol reveals memory deficits at 4-months of age in the triple-transgenic mouse model of Alzheimer's disease. PloS one 8, e80355.
Banerjee, S. B., Gutzeit, V. A., Baman, J., Aoued, H. S., Doshi, N. K., Liu, R. C., Ressler, K. J., 2017. Perineuronal nets in the adult sensory cortex are necessary for fear learning. Neuron 95, 169-179.
Bertocchi, I., Oberto, A., Longo, A., Mele, P., Sabetta, M., Bartolomucci, A., Palanza, P., Sprengel, R., Eva, C., 2011. Regulatory functions of limbic Y1 receptors in body weight and anxiety uncovered by conditional knockout and maternal care. Proc Natl Acad Sci U S A 108, 19395-19400.
Bertocchi, I., Oberto, A., Longo, A., Palanza, P., Eva, C., 2020. Conditional inactivation of Npy1r gene in mice induces sex-related differences of metabolic and behavioral functions. Hormones and Behavior 125, 104824.
Blacktop, J. M., Todd, R. P., Sorg, B. A., 2017. Role of perineuronal nets in the anterior dorsal lateral hypothalamic area in the acquisition of cocaine-induced conditioned place preference and self-administration. Neuropharmacology 118, 124-136.
Bozzelli, P.L., Alaiyed, S., Kim, E., Villapol, S., Conant, K., 2018. Proteolytic remodeling of perineuronal nets: effects on synaptic plasticity and neuronal population dynamics. Neural plasticity 2018:5735789.
Carstens, K. E., Phillips, M. L., Pozzo-Miller, L., Weinberg, R. J., Dudek, S. M., 2016. Perineuronal nets suppress plasticity of excitatory synapses on CA2 pyramidal neurons. Journal of Neuroscience 36, 6312-6320.
Carulli, D., Pizzorusso, T., Kwok, J. C. F., Putignano, E., Poli, A., Forostyak, S., Andrews, M. R., Deepa, S. S., Glant, T. T., Fawcett, J. W., 2010. Animals lacking link protein have attenuated perineuronal nets and persistent plasticity. Brain 133, 2331-2347.
Carulli, D., Broersen, R., de Winter, F., Muir, E. M., Mešković, M., de Waal, M., de Vries, S., Boele, H.-J., Canto, C. B., De Zeeuw, C. I., 2020. Cerebellar plasticity and associative memories are controlled by perineuronal nets. Proceedings of the National Academy of Sciences 117, 6855-6865.
Cattaud, V., Bezzina, C., Rey, C. C., Lejards, C., Dahan, L., Verret, L., 2018. Early disruption of parvalbumin expression and perineuronal nets in the hippocampus of the Tg2576 mouse model of Alzheimer's disease can be rescued by enriched environment. Neurobiology of aging 72, 147-158.
Crespo, D., Asher, R. A., Lin, R., Rhodes, K. E., Fawcett, J. W., 2007. How does chondroitinase promote functional recovery in the damaged CNS? Experimental neurology 206, 159-171.
Dayan, E., Censor, N., Buch, E. R., Sandrini, M., Cohen, L. G., 2013. Noninvasive brain stimulation: from physiology to network dynamics and back. Nature neuroscience 16, 838-844.
Donato, F., Chowdhury, A., Lahr, M., Caroni, P., 2015. Early-and late-born parvalbumin basket cell subpopulations exhibiting distinct regulation and roles in learning. Neuron 85, 770-786.
Eaton, K., Sallee, F. R., Sah, R., 2007. Relevance of neuropeptide Y (NPY) in psychiatry. Current topics in medicinal chemistry 7, 1645-1659.
Enman, N. M., Sabban, E. L., McGonigle, P., Van Bockstaele, E. J., 2015. Targeting the neuropeptide Y system in stress-related psychiatric disorders. Neurobiology of stress 1, 33-43.
Eva, C., Serra, M., Mele, P., Panzica, G., Oberto, A., 2006. Physiology and gene regulation of the brain NPY Y1 receptor. Frontiers in neuroendocrinology 27, 308-339.
Fawcett, J. W., Oohashi, T., Pizzorusso, T., 2019. The roles of perineuronal nets and the perinodal extracellular matrix in neuronal function. Nature reviews Neuroscience 20, 451-465.
Foscarin, S., Ponchione, D., Pajaj, E., Leto, K., Gawlak, M., Wilczynski, G. M., Rossi, F., Carulli, D., 2011. Experience-dependent plasticity and modulation of growth regulatory molecules at central synapses. PloS one 6, e16666.

Froemke, R. C., Schreiner, C. E., 2015. Synaptic plasticity as a cortical coding scheme. Current opinion in neurobiology 35, 185-199.
Geissler, M., Gottschling, C., Aguado, A., Rauch, U., Wetzel, C. H., Hatt, H., Faissner, A., 2013. Primary hippocampal neurons, which lack four crucial extracellular matrix molecules, display abnormalities of synaptic structure and function and severe deficits in perineuronal net formation. Journal of neuroscience 33, 7742-7755.
Gogolla, N., Caroni, P., Lüthi, A., Herry, C., 2009. Perineuronal nets protect fear memories from erasure. Science 325, 1258-1261.
Gutman, A. R., Yang, Y., Ressler, K. J., Davis, M., 2008. The role of neuropeptide Y in the expression and extinction of fear-potentiated startle. Journal of Neuroscience 28, 12682-12690.
Gøtzsche, C. R., Woldbye, D. P. D., 2016. The role of NPY in learning and memory. Neuropeptides 55, 79-89.
Hadad-Ophir, O., Albrecht, A., Stork, O., Richter-Levin, G., 2014. Amygdala activation and GABAergic gene expression in hippocampal sub-regions at the interplay of stress and spatial learning. Frontiers in behavioral neuroscience 8, 3.
Hamilton, T. J., Wheatley, B. M., Sinclair, D. B., Bachmann, M., Larkum, M. E., Colmers, W. F., 2010. Dopamine modulates synaptic plasticity in dendrites of rat and human dentate granule cells. Proceedings of the National Academy of Sciences 107, 18185-18190.
Happel, M. F. K., Niekisch, H., Rivera, L. L. C., Ohl, F. W., Deliano, M., Frischknecht, R., 2014. Enhanced cognitive flexibility in reversal learning induced by removal of the extracellular matrix in auditory cortex. Proceedings of the National Academy of Sciences 111, 2800-2805.
Harrison, F. E., Hosseini, A. H., McDonald, M. P., 2009. Endogenous anxiety and stress responses in water maze and Barnes maze spatial memory tasks. Behavioural brain research 198, 247-251.
Hei, Y., Wei, L., Yi, X., Liu, W., Long, Q., 2018. Parvalbumin and Neuropeptide Y Neuronal Loss in the Hippocampal CA1 Subarea is Associated with Cognitive Deficits in a Rat Model of Chronic Cerebral Hypoperfusion. Neuropsychiatry 8, 293-301.
Hirono, M., Watanabe, S., Karube, F., Fujiyama, F., Kawahara, S., Nagao, S., Yanagawa, Y., Misonou, H., 2018. Perineuronal nets in the deep cerebellar nuclei regulate GABAergic transmission and delay eyeblink conditioning. Journal of Neuroscience 38, 6130-6144.
Horii-Hayashi, N., Sasagawa, T., Matsunaga, W., Nishi, M., 2015. Development and structural variety of the chondroitin sulfate proteoglycans-contained extracellular matrix in the mouse brain. Neural plasticity. 2015:256389.
Hylin, M. J., Orsi, S. A., Moore, A. N., Dash, P. K., 2013. Disruption of the perineuronal net in the hippocampus or medial prefrontal cortex impairs fear conditioning. Learning & Memory 20, 267-273.
Härtig, W., Brauer, K., Brückner, G., 1992. Wisteria floribunda agglutinin-labelled nets surround parvalbumin-containing neurons. Neuroreport 3, 869-872.
Hörmer, B. A., Verma, D., Gasser, E., Wieselthaler-Hölzl, A., Herzog, H., Tasan, R. O., 2018. Hippocampal NPY Y2 receptors modulate memory depending on emotional valence and time. Neuropharmacology 143, 20-28.
Jazmati, D., Neubacher, U., Funke, K., 2018. Neuropeptide Y as a possible homeostatic element for changes in cortical excitability induced by repetitive transcranial magnetic stimulation. Brain stimulation 11, 797-805.
Karagiannis, A., Gallopin, T., Dávid, C., Battaglia, D., Geoffroy, H., Rossier, J., Hillman, E. M. C., Staiger, J. F., Cauli, B., 2009. Classification of NPY-expressing neocortical interneurons. Journal of Neuroscience 29, 3642-3659.
Kovacs, K. J., 2008. Measurement of immediate-early gene activation-c-fos and beyond. Journal of neuroendocrinology 20, 665-672.
Kwok, J. C. F., Dick, G., Wang, D., Fawcett, J. W., 2011. Extracellular matrix and perineuronal nets in CNS repair. Developmental neurobiology 71, 1073-1089.
Lach, G., de Lima, T. C. M., 2013. Role of NPY Y1 receptor on acquisition, consolidation and extinction on contextual fear conditioning: dissociation between anxiety, locomotion and non-emotional memory behavior. Neurobiology of learning and memory 103, 26-33.

Lapray, D., Lasztoczi, B., Lagler, M., Viney, T. J., Katona, L., Valenti, O., Hartwich, K., Borhegyi, Z., Somogyi, P., Klausberger, T., 2012. Behavior-dependent specialization of identified hippocampal interneurons. Nature neuroscience 15, 1265-1271.
Lensjø, K. K., Lepperød, M. E., Dick, G., Hafting, T., Fyhn, M., 2017. Removal of perineuronal nets unlocks juvenile plasticity through network mechanisms of decreased inhibition and increased gamma activity. Journal of Neuroscience 37, 1269-1283.
Lenz, M., Galanis, C., Müller-Dahlhaus, F., Opitz, A., Wierenga, C. J., Szabó, G., Ziemann, U., Deller, T., Funke, K., Vlachos, A., 2016. Repetitive magnetic stimulation induces plasticity of inhibitory synapses. Nature communications 7, 1-13.
Letzkus, J. J., Wolff, S. B. E., Lüthi, A., 2015. Disinhibition, a circuit mechanism for associative learning and memory. Neuron 88, 264-276.
Loh, K., Herzog, H., Shi, Y.-C., 2015. Regulation of energy homeostasis by the NPY system. Trends in Endocrinology & Metabolism 26, 125-135.
Longo, A., Fadda, M., Brasso, C., Mele, P., Palanza, P., Nanavaty, I., Bertocchi, I., Oberto, A., Eva, C., 2018. Conditional inactivation of Npy1r gene in mice induces behavioural inflexibility and orbitofrontal cortex hyperactivity that are reversed by escitalopram. Neuropharmacology 133, 12-22.
Longo, A., Mele, P., Bertocchi, I., Oberto, A., Bachmann, A., Bartolomucci, A., Palanza, P., Sprengel, R., Eva, C., 2014. Conditional inactivation of neuropeptide Y Y1 receptors unravels the role of Y1 and Y5 receptors coexpressing neurons in anxiety. Biol Psychiatry 76, 840-849.
Marrone, D. F., Schaner, M. J., McNaughton, B. L., Worley, P. F., Barnes, C. A., 2008. Immediate-early gene expression at rest recapitulates recent experience. Journal of Neuroscience 28, 1030-1033.
O'Keefe, J., Dostrovsky, J., 1971. The hippocampus as a spatial map: preliminary evidence from unit activity in the freely-moving rat. Brain research 34, 171-175.
Oberto, A., Panzica, G. C., Altruda, F., Eva, C., 2001. GABAergic and NPY-Y1 network in the medial amygdala: a neuroanatomical basis for their functional interaction. Neuropharmacology 41, 639-642.
Ohline, S. M., Wake, K. L., Hawkridge, M. V., Dinnunhan, M. F., Hegemann, R. U., Wilson, A., Schoderboeck, L., Logan, B. J., Jungenitz, T., Schwarzacher, S. W., 2018. Adult-born dentate granule cell excitability depends on the interaction of neuron age, ontogenetic age and experience. Brain Structure and Function 223, 3213-3228.
Pantazopoulos, H., Berretta, S., 2016. In sickness and in health: perineuronal nets and synaptic plasticity in psychiatric disorders. Neural plasticity 2016:9847696.
Pizzorusso, T., Medini, P., Berardi, N., Chierzi, S., Fawcett, J. W., Maffei, L., 2002. Reactivation of ocular dominance plasticity in the adult visual cortex. Science 298, 1248-1251.
Rangani, R. J., Upadhya, M. A., Nakhate, K. T., Kokare, D. M., Subhedar, N. K., 2012. Nicotine evoked improvement in learning and memory is mediated through NPY Y1 receptors in rat model of Alzheimer's disease. Peptides 33, 317-328.
Reibel, S., Vivien-Roels, B., Lê, B. T., Larmet, Y., Carnahan, J., Marescaux, C., Depaulis, A., 2000. Overexpression of neuropeptide Y induced by brain-derived neurotrophic factor in the rat hippocampus is long lasting. European Journal of Neuroscience 12, 595-605.
Reichmann, F., Holzer, P., 2016. Neuropeptide Y: A stressful review. Neuropeptides 55, 99-109.
Reichmann, F., Wegerer, V., Jain, P., Mayerhofer, R., Hassan, A. M., Fröhlich, E. E., Bock, E., Pritz, E., Herzog, H., Holzer, P., 2016. Environmental enrichment induces behavioural disturbances in neuropeptide Y knockout mice. Scientific reports 6, 28182.
Ridding, M. C., Ziemann, U., 2010. Determinants of the induction of cortical plasticity by non-invasive brain stimulation in healthy subjects. The Journal of physiology 588, 2291-2304.
Riga, D., Kramvis, I., Koskinen, M. K., Van Bokhoven, P., Van Der Harst, J. E., Heistek, T. S., Timmerman, A. J., Van Nierop, P., Van Der Schors, R. C., Pieneman, A. W., 2017. Hippocampal extracellular matrix alterations contribute to cognitive impairment associated with a chronic depressive-like state in rats. Science Translational Medicine 9.
Romberg, C., Yang, S., Melani, R., Andrews, M. R., Horner, A. E., Spillantini, M. G., Bussey, T. J., Fawcett, J. W., Pizzorusso, T., Saksida, L. M., 2013. Depletion of perineuronal nets enhances recognition memory and long-term depression in the perirhinal cortex. Journal of Neuroscience 33, 7057-7065.

Rowlands, D., Lensjø, K. K., Dinh, T., Yang, S., Andrews, M. R., Hafting, T., Fyhn, M., Fawcett, J. W., Dick, G., 2018. Aggrecan directs extracellular matrix-mediated neuronal plasticity. Journal of Neuroscience 38, 10102-10113.
Sale, A., Vetencourt, J. F. M., Medini, P., Cenni, M. C., Baroncelli, L., De Pasquale, R., Maffei, L., 2007. Environmental enrichment in adulthood promotes amblyopia recovery through a reduction of intracortical inhibition. Nature neuroscience 10, 679-681.
Seol, G. H., Ziburkus, J., Huang, S., Song, L., Kim, I. T., Takamiya, K., Huganir, R. L., Lee, H. K., Kirkwood, A., 2007. Neuromodulators control the polarity of spike-timing-dependent synaptic plasticity. Neuron 55, 919-929.
Shi, W., Wei, X., Wang, X., Du, S., Liu, W., Song, J., Wang, Y., 2019. Perineuronal nets protect long-term memory by limiting activity-dependent inhibition from parvalbumin interneurons. Proceedings of the National Academy of Sciences 116, 27063-27073.
Shimshek, D. R., Jensen, V., Celikel, T., Geng, Y., Schupp, B., Bus, T., Mack, V., Marx, V., Hvalby, Ø., Seeburg, P. H., 2006. Forebrain-specific glutamate receptor B deletion impairs spatial memory but not hippocampal field long-term potentiation. Journal of Neuroscience 26, 8428-8440.
Sigal, Y. M., Bae, H., Bogart, L. J., Hensch, T. K., Zhuang, X., 2019. Structural maturation of cortical perineuronal nets and their perforating synapses revealed by superresolution imaging. Proceedings of the National Academy of Sciences 116, 7071-7076.
Silva, A. J., Simpson, E. M., Takahashi, J. S., Lipp, H.-P., Nakanishi, S., Wehner, J. M., Giese, K. P., Tully, T., Abel, T., Chapman, P. F., 1997. Mutant mice and neuroscience: recommendations concerning genetic background. Neuron 19, 755-759.
Slaker, M., Churchill, L., Todd, R. P., Blacktop, J. M., Zuloaga, D. G., Raber, J., Darling, R. A., Brown, T. E., Sorg, B. A., 2015. Removal of perineuronal nets in the medial prefrontal cortex impairs the acquisition and reconsolidation of a cocaine-induced conditioned place preference memory. Journal of Neuroscience 35, 4190-4202.
Stanić, D., Mulder, J., Watanabe, M., Hökfelt, T., 2011. Characterization of NPY Y2 receptor protein expression in the mouse brain. II. Coexistence with NPY, the Y1 receptor, and other neurotransmitter-related molecules. Journal of Comparative Neurology 519, 1219-1257.
Thompson, E. H., Lensjø, K. K., Wigestrand, M. B., Malthe-Sørenssen, A., Hafting, T., Fyhn, M., 2018. Removal of perineuronal nets disrupts recall of a remote fear memory. Proceedings of the National Academy of Sciences 115, 607-612.
Vollmer, L. L., Schmeltzer, S., Schurdak, J., Ahlbrand, R., Rush, J., Dolgas, C. M., Baccei, M. L., Sah, R., 2016. Neuropeptide Y Impairs Retrieval of Extinguished Fear and Modulates Excitability of Neurons in the Infralimbic Prefrontal Cortex. The Journal of Neuroscience 36, 1306-1315.
Whishaw, I. Q., Tomie, J.-A., 1996. Of mice and mazes: similarities between mice and rats on dry land but not water mazes. Physiology & behavior 60, 1191-1197.
Xue, Y.-X., Xue, L.-F., Liu, J.-F., He, J., Deng, J.-H., Sun, S.-C., Han, H.-B., Luo, Y.-X., Xu, L.-Z., Wu, P., 2014. Depletion of perineuronal nets in the amygdala to enhance the erasure of drug memories. Journal of Neuroscience 34, 6647-6658.
Yamada, J., Jinno, S., 2013. Spatio-temporal differences in perineuronal net expression in the mouse hippocampus, with reference to parvalbumin. Neuroscience 253, 368-379.
Ziemann, U., Siebner, H. R., 2008. Modifying motor learning through gating and homeostatic metaplasticity. Brain stimulation 1, 60-66.

Figure legends

Figure 1. Npy1r^{rfb} mice display decreased spatial learning in the Morris water maze and in the Barnes maze. (**A**) MWM acquisition phase. Npy1r^{rfb} mice show increased latency to reach the platform over 4 days of training compared to Npy1r^{2lox} mice. (**B**) Barnes maze acquisition phase. Npy1r^{rfb} mice spend more time to reach the target hole over 4 days of training compared to Npy1r^{2lox} mice. (**C** and **D**) Probe trials. After training, the platform (MWM) and the escape box (Barnes maze) were removed from the south west quadrant (Target) where they were originally placed. The y axis indicates the percentage of time spent in each quadrant. Data are the mean ± SEM. (**E**) Swimming paths during the MWM acquisition phase show the learning delay of Npy1r^{rfb} mice.

MWM, Morris water maze; SW, south west; SE, south east; NE, north east; NW, north west.

Figure 2. Npy1r^{rfb} mice display increased perineuronal nets intensity in the CA1 region of the hippocampus. WFA+ (**A**) and aggrecan+ (**B**) PNNs in the in the stratum pyramidalis (s.p.) and the stratum oriens (s.o.) of the CA1 of Npy1r^{2lox} and Npy1r^{rfb} mice. Scale bar: 100 µm. **C** and **D** show the frequency distribution of weak, medium or strongly stained WFA+ and aggrecan+ PNNs, respectively. ***p<0.001; *p< 0.05. WFA, *Wisteria floribunda agglutinin*; NeuN, neuronal nuclear antigene.

Figure 3. Perineuronal nets intensity is increased around both parvalbumin positive and negative neurons in the CA1 of Npy1r^{rfb} mice.

WFA+ PNNs around PV^{+} (**A**, white arrow) and PV^{-} (**B**, yellow arrow head) neurons in the CA1 of Npy1r^{2lox} and Npy1r^{rfb} mice. Scale bar: 100 µm. **C** and **D** show the frequency distribution of weak, medium or strongly stained WFA+ PNNs around PV+ and PV- cells, respectively, in the stratum pyramidalis (s.p.) and the stratum oriens (s.o.). ***p<0.001; **p=0.01. PV, parvalbumin.

Figure 4. Npy1r^{rfb} mice show increased perineuronal net coating complexity in the CA1.

(**A**) Representative picture of Sholl analysis of WFA+ PNNs coating around dendrites of NeuN labelled neurons in the stratum pyramidalis (s.p) of the CA1 of Npy1r^{2lox} and Npy1r^{rfb} mice. Scale bar: 100 µm. (**B**) Analysis of the number of 10 µm spaced concentric ring intersections (left panel) and of the sum of the length of inter-rings segments (length, right panel) in the CA1. *p<0.05 by Newman Keuls. (**C**) Analysis of the

number of ring intersections (left panel) and of length of inter-rings segments in the stratum oriens (s.o.) of the CA1. *p<0.05 by Newman Keuls. (**D**) The analysis of the number of ring intersections (left panel) and of the sum of the length of inter-rings segments (right panel) in the stratum radiatum (s.r.) reveals no significant differences between Npy1r^{rfb} mice and their control littermates.

Figure 5. Perineuronal nets digestion rescues learning ability of Npy1r^{rfb} mice.

(**A**) Timeline of the experiment. Saline or ChABC were delivered in the dorsal hippocampus in order to digest PNNs located in the CA1. Animals were allowed to recover for three days and then subjected to the MWM or Barnes maze tests for spatial memory. (**B**) WFA staining of brain coronal sections from saline or ChABC-treated Npy1r^{rfb} mice. Magnification of boxed area shows that ChABC injection removes PNNs in the CA1. Scale bar, 2mm. (**C**) Acquisition phase in the MWM. ***p<0.001 versus saline treated Npy1r^{2lox} mice and ChABC treated Npy1r^{rfb} mice; **p<0.01 vs ChABC treated Npy1r^{2lox} mice by Newman Keuls. (**D**) Acquisition phase in the Barnes test. ***p<0.001 versus saline and ChABC treated Npy1r^{2lox} mice; **p<0.01 and +p=0.087 vs ChABC treated Npy1r^{rfb} mice on the 4th and 3rd day of training, respectively; **p<0.01 versus saline treated Npy1r^{2lox} mice on the 3rd day of training and **p<0.01 versus saline treated Npy1r^{2lox} mice on the 2nd day of training by Newman Keuls. (**E** and **F**) Probe trials. After training, the platform (MWM) and the escape box (Barnes maze) were removed from the south west quadrant (Target) where they were originally placed. The y axis indicates the percentage of time spent in each quadrant. Data are the mean ± SEM. ChABC, chondroitinase ABC; SW, south west; SE, south east; NE, north east; NW, north west.

Figure 6. PNNs digestion rescues overexcitation in the stratum pyramidalis of the CA1 of Npy1r^{rfb} mice.

(**A**) Double immunofluorescence staining with anti c-Fos (white), anti parvalbumin (PV, green) and merged signals in slices of CA1 stratum pyramidalis from control and Npy1r^{rfb} mutant mice treated with saline. Scale bar: 100 µm. (**B**) Quantification of c-Fos+ cells in the stratum pyramidalis of CA1 in both saline and ChABC-injected Npy1r^{2lox} and Npy1r^{rfb} mice. *p<0.05 versus saline treated Npy1r^{2lox} mice and **p<0.01 versus ChABC-injected Npy1r^{rfb} mice. Data are the mean ± SEM; n=4-5 from 5 litters.

Table 1. Colocalization of WFA, PV and NeuN in hippocampal slices of Npy1r^{2lox} and Npy1r^{rfb} mice. No significant differences between genotypes were found for any of the markers analyzed. s.p.: stratum pyramidalis; s.o. stratum oriens; s.gr: stratum granulare; WFA: *Wisteria floribunda agglutinin*; PV:parvalbumin; NeuN: neuronal nuclear antigen.

	CA1 s.p.		CA1 s.o.		CA3 s.p.		DG s.gr	
	Npy1r^{2lox}	Npy1r^{rfb}	Npy1r^{2lox}	Npy1r^{rfb}	Npy1r^{2lox}	Npy1r^{rfb}	Npy1r^{2lox}	Npy1r^{rfb}
Percentage of WFA$^+$/PV$^+$	82.3±5.12	70.5±7.40	85.3±5.44	85.0±5.04	86.9±5.65	9 1.4±3.56	86.0±3.26	88.9±4.38
Percentage of WFA$^+$/PV$^-$	17.7±5.13	29.3±7.48	14.7±5.44	15.6±4.81	13.1±5.65	8 .58±3.56	14.0±3.2	11.1±4.38
Percentage of PV$^+$/WFA$^+$	60.9±5.45	60.7±5.01	73.4±6.81	70.3±6.79	51.8±4.07	5 4.9±4.27	78.3±3.52	75.1±3.49
Percentage of NeuN$^+$/WFA$^+$	1.9±0.21	2.3±0.36	19.5±3.84	21.1±6.20	2.8±0.35	3.3± 0.32	0.35±0.05	0.50±0.06
Percentage of NeuN$^+$/PV$^+$	2.1±0.27	2.7±0.39	23.7±2.91	34.2±7.60	2.7±0.35	3.4± 0.34	0.28±0.05	0.46±0.09

Table 2. Colocalization of c-Fos, PV and DAPI in hippocampal slices of Npy1r^{2lox} and Npy1r^{rfb} mice. Percentage of colocalization of c-Fos and DAPI and percentage of c-Fos^{+}/PV^{+} cells on the total number of c-Fos^{+} cells in the stratum pyramidalis (s.p.) of CA1 of Npy1r^{2lox} and Npy1r^{rfb} mice. $^{a}p<0.05$ versus saline treated Npy1r^{2lox} mice and $^{b}p<0.01$ versus ChABC-injected Npy1r^{rfb} mice. Data are the mean ± SEM; n=4-5 from 5 litters. PV: parvalbumin; DAPI: 4′,6-diamidino-2-phenylindole, nuclear stain.

	CA1 s.p.			
	Npy1r^{2lox} saline	Npy1r^{rfb} saline	Npy1r^{2lox} ChABC	Npy1r^{rfb} ChABC
Percentage of c-Fos^{+}/DAPI	4.86±5.12	8.25±1.22^{a,b}	5.76±0.55	3.52±1.03
Percentage of PV^{+}c-Fos^{+}/c-Fos^{+}	6.54±1.91	3.04±0.46	9.69±1.34	10.1±3.26

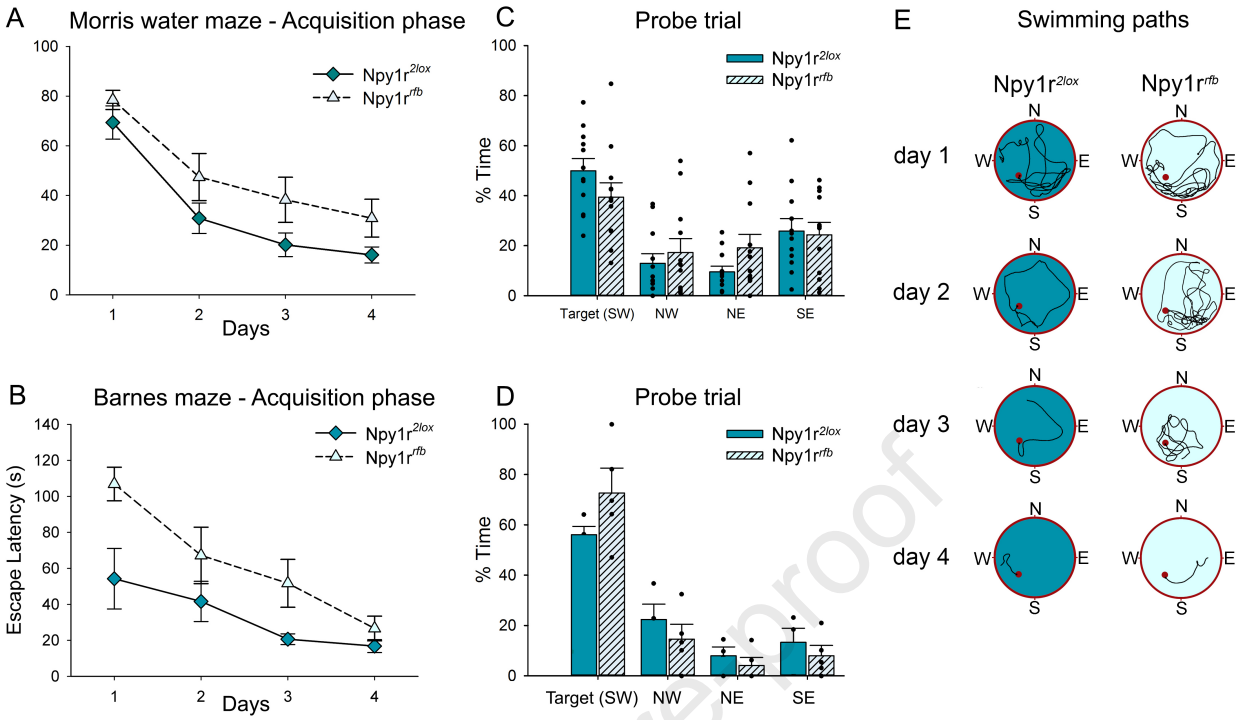

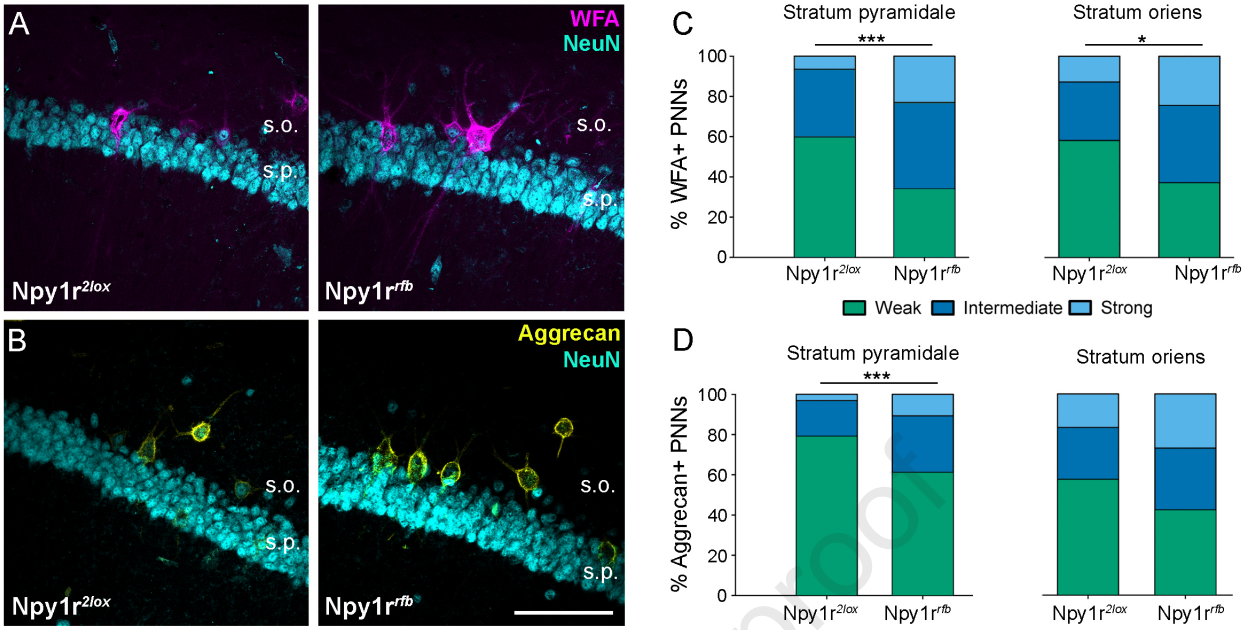

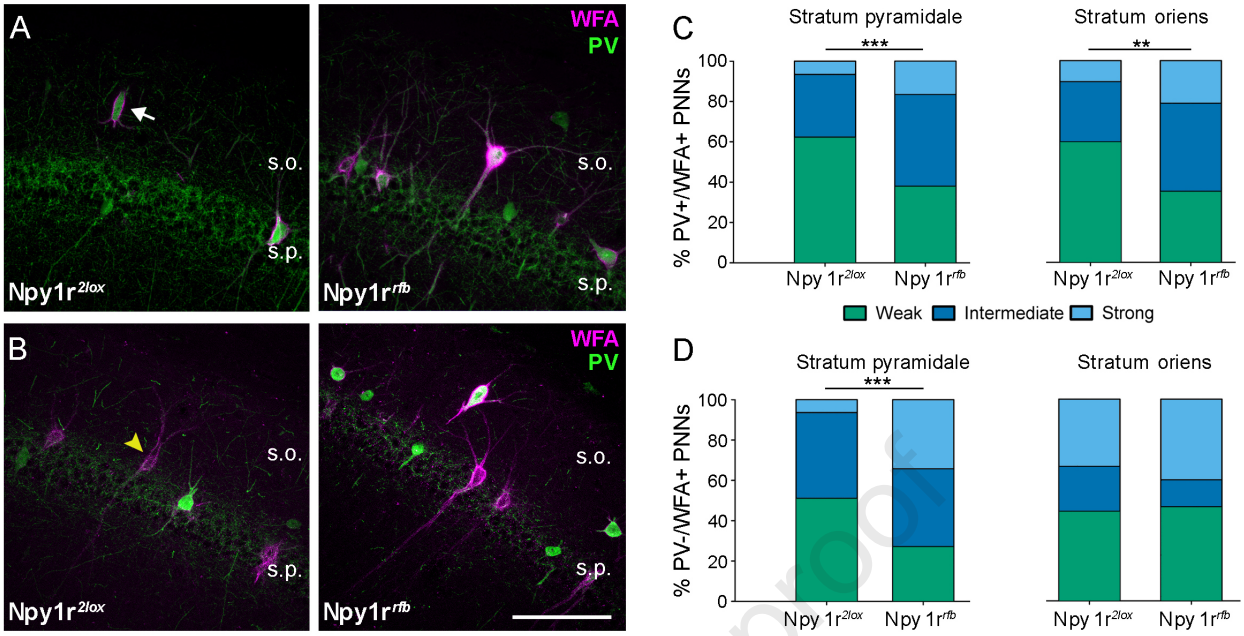

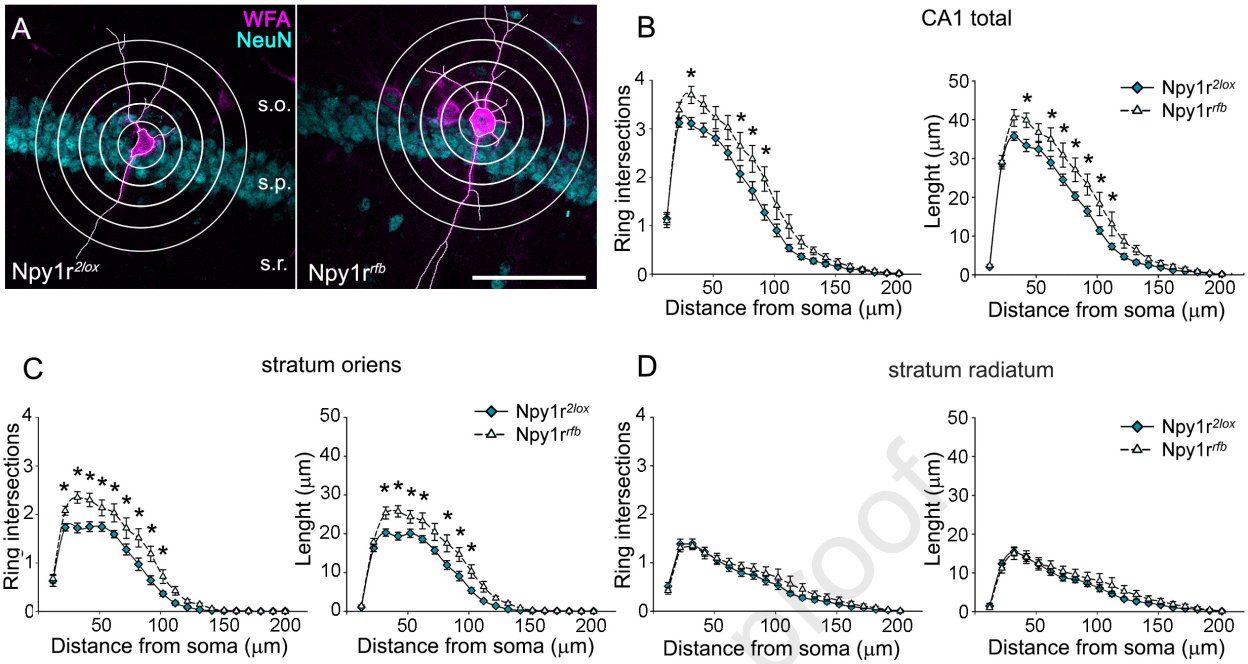

Effect of perineuronal nets digestion on spatial learning of control and mutant mice

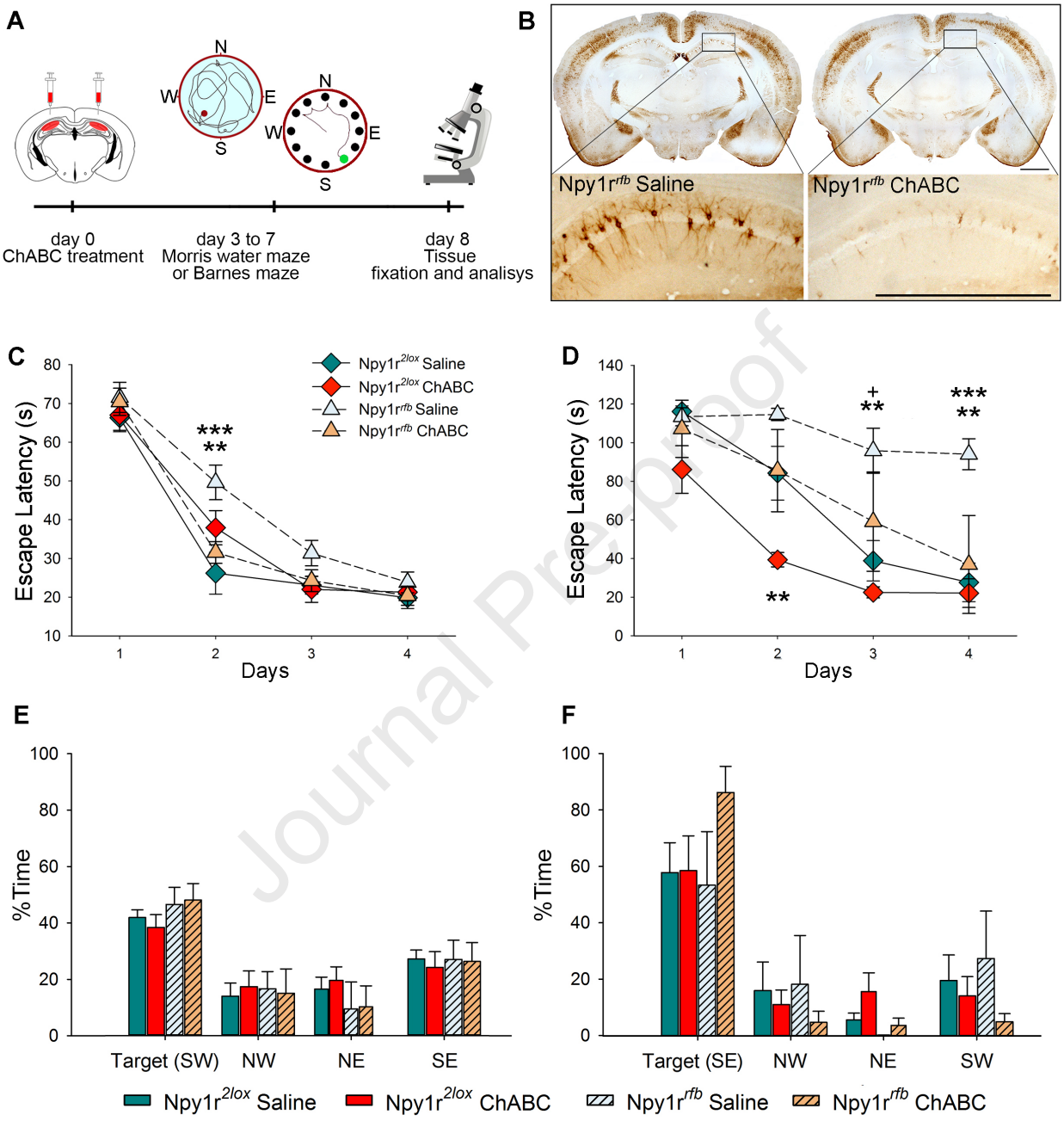

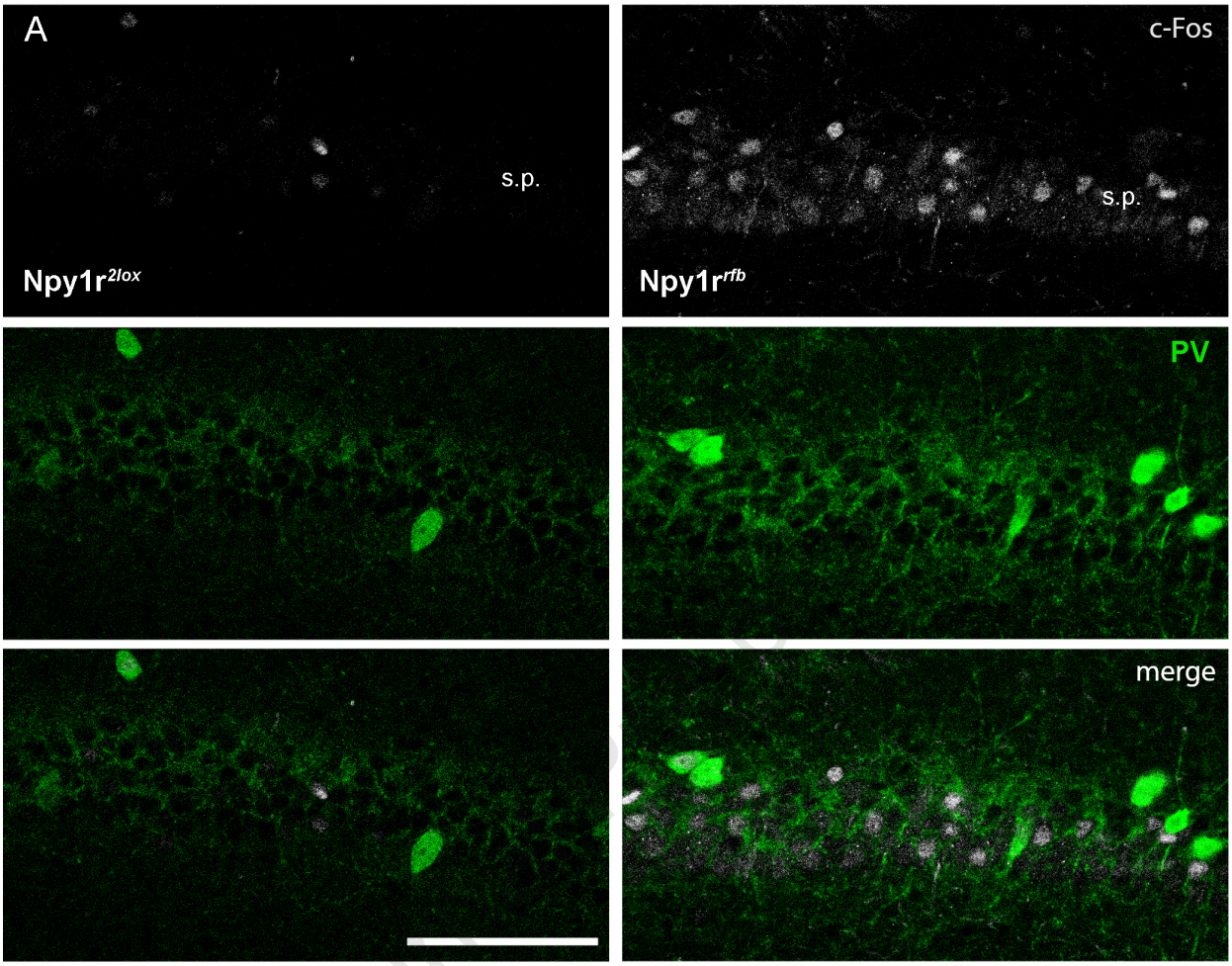
A
s.p.
Npy1r2lox
c-Fos
s.p.
Npy1rrfb
PV
merge

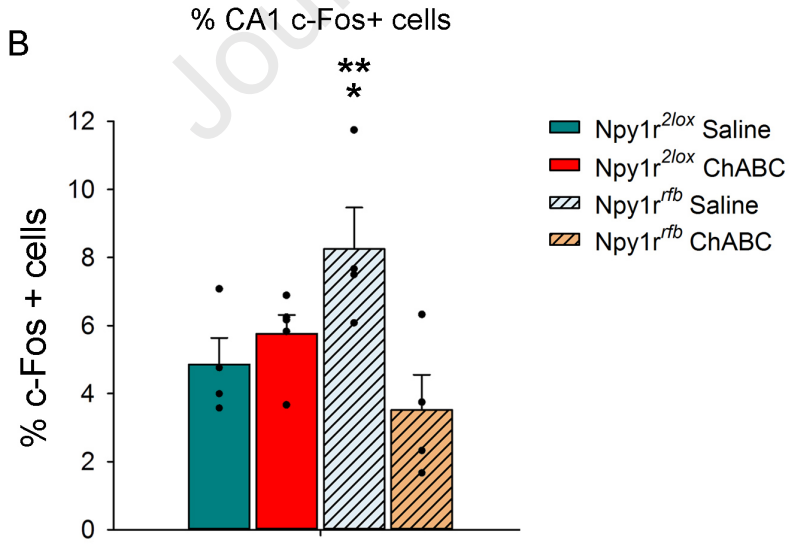
B
% CA1 c-Fos+ cells
**
*
% c-Fos + cells
12
10
8
6
4
2
0
Npy1r2lox Saline
Npy1r2lox ChABC
Npy1rrfb Saline
Npy1rrfb ChABC

Highlights

- Y1R knockout impairs learning, increases PNN intensity and c-Fos activity in the CA1
- PNN enzymatic digestion rescues learning abilities and normalizes c-Fos activity
- NPY facilitates learning possibly by modulating PNN expression and CA1 excitability